

## Proton-proton pair correlation and properties of the emitting source at Fermi energy

---

**E. V. Pagano\***

*Universita' di Catania, INFN-LNS*

*E-mail: [epagano@lns.infn.it](mailto:epagano@lns.infn.it)*

**T. Minniti**

*Universita' di Catania, INFN-Sezione di Catania*

**B. Barker**

*Michigan State University - NSCL*

The study of the dynamics of nuclear reactions in heavy ion collisions is a very interesting topic in nuclear physics. This study is strongly related with crucial open problems. Among them we mention the isospin dependence of the Equation of State in asymmetric nuclear matter, the existence of a liquid-gas phase transitions in nuclei, the characterization of exotic nuclear systems. A clear understanding of the effective interaction in nuclei requires the evaluation of the space-time properties of the reaction mechanism along with related properties of the various sources of particle emission which are involved. Correlations between like as well as unlike-particles are very powerful techniques to study the properties of the emitting sources that are involved in the different stages of a reaction. In this work we have studied two-proton correlation functions measured in Xe+Au at E=50 MeV/nucleon. By using angle-averaged two proton correlation functions and an "imaging" analysis technique we have studied some basic proprieties (size, lifetimes, intensity) of the emitting source functions of proton-proton pairs in semi-central collisions.

*International Winter Meeting on Nuclear Physics,  
21-25 January 2013  
Bormio, Italy*

---

\*Speaker.

## 1. Introduction

Understanding the dynamics of nuclear reactions in heavy ion collisions is a very attractive topic in nuclear physics. Large efforts have been devoted to study the competition among different reaction mechanisms leading to quite similar asymptotic channels. In fact, depending on the beam energy, one is faced with different time-scales of the response of the nucleus to the excitation of the relevant (energy dependent) degrees of freedom. Moreover, the effective nuclear many body interaction acting among the participant nucleons in the most violent collisions opens the possibility to explore short-lived nuclear systems with densities lower or larger than the one of nuclear matter at saturation ( $\rho_0 = 0.17 \text{ nucleon}/\text{fm}^3$ ). In particular, at intermediate energies, between 20 MeV/u and 200 MeV/u, within time-scales of the order of 100 fm/c, the dynamical phase of a violent head-on collision experiences a collective compression where the overlapping nuclear density is predicted [1, 2] to achieve values above the value of the saturation density. Then, the evolution of this strong interacting participant zone is predicted to undergo an expansion phase where the nuclear density decreases to significant lower value than the saturation density (of the order of  $0.3\rho_0$ , the so-called, freeze-out phase) and consequently, within a short time scale ( $< 100$  fm/c), a rapid multi-fragmentation of the diluted system in many excited clusters and light particle may take place. It is still a fundamental open question if at freeze-out the system achieves full equilibrium or not. However, clear evidence of secondary decays coming from excited fragments has been established [3, 4, 5]. It is within this very complex reaction scenario that experimental methods and techniques for probing space-time property of the different emitting sources have been developed. Among the various techniques introduced in nuclear science in order to probe the different phases of the reaction (from the early dynamical phase to the full equilibrium one) correlation functions and intensity interferometry play a key role [6]. In the following sections, the basic properties of the particle correlation techniques will be briefly summarized and applied to the study of a specific nuclear reaction.

## 2. Experimental method

Early in nuclear reaction studies, scientists were faced with the crucial problem to disentangle among different time-scales of the reaction that are involved in the same collision process [7]. Indeed, in order to well understand properties of the in medium nuclear interaction one has to take into account, in a consistent way, the whole time scale involved in the reaction, i.e, from the prompt particle emissions that are created during the collision dynamics (few fm/c) to the ones that are sequentially evaporated over time-scales orders of magnitude longer than the prompt ones. However, taking into account for the different stages of the collision along with the associated different emitting sources of particles is a real experimental challenge. Moreover, from a theoretical point of view, it is well known, at intermediate energies, the dynamic of the reaction depends on the nuclear mean field transport properties determined by the effective nucleon-nucleon interaction. In determining the reaction pattern, crucial parameters are the incident energy of the beam, the centrality of the collision (impact parameter), the mass and the charge of the interacting binary systems. In this work special attention is paid to the Fermi Energy domain (around 50 AMeV) where strong completion between mean field and nucleon-nucleon collisions are expected to determine the re-

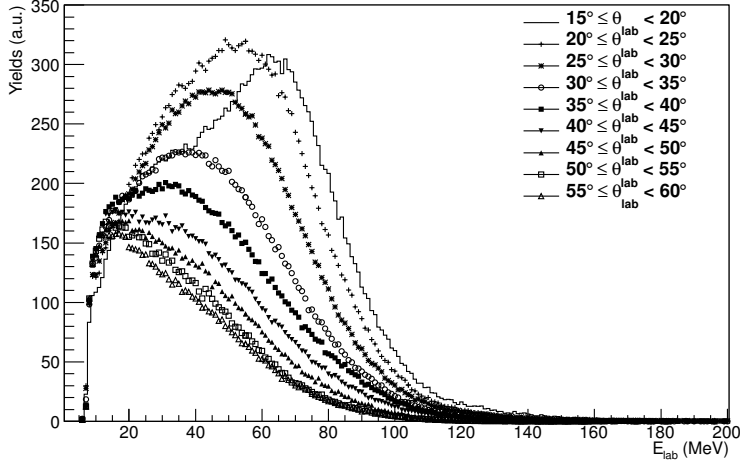


**Figure 1:** Protons energy spectra for different angular regions in lab frame for all  $Mult_{tot}$

action scenario. In particular, the present study is devoted to select quasi-central collisions in the reaction  $^{129}\text{Xe} + ^{197}\text{Au}$  at  $E/A=50$  MeV/u. The experimental interferometry analysis concerns with data collected in an experiment that was performed at Michigan State University (MSU) and the experimental setup was composed of LASSA, that is an array of nine telescopes, each consisting of two stages of Double Sided Silicon Strip Detector (DSSSD) and four CsI(Tl) crystals, coupled to the Miniball/Miniwall array, more details about the experimental setup are available in Ref. [8]. A preliminary analysis of the data has been discussed in preliminary works [12, 14], a brief summary of the experimental results is given in the following. Central collision events were selected by using the total charged particle multiplicity ( $Mult_{tot}$ ), that is the sum of the number of charged particles detected in LASSA plus the number of charged particles detected in the Miniball/Miniwall. By studying proton energy spectra, it was observed that for  $Mult_{tot} < 30$  (quasi-peripheral collisions events) the spectra showed a strong contribution of a fast component at forward laboratory angles between  $12^\circ$  and  $14^\circ$ ; in fact a broad bump was clearly observed, ranging roughly between 60 and 90 MeV, and peaked to a value of about 70 MeV, corresponding to a value of proton velocity which is about 14% larger than the velocity of the beam. This component may contain contributions from protons emitted at the early stage of the reaction (fast emission) and protons emitted by quasi-projectile evaporations (slow emissions) [12, 14]. We noticed that the presence of the bump is strongly reduced by selecting the most violent collisions when analysing spectra with high values of the particle multiplicity, i.e.,  $Mult_{tot} > 30$ . This may indicated that the bump originate mostly from quasi-projectile emissions. In Fig.1 the overall obtained energy distribution is reported in the angle range between  $15^\circ$  and  $60^\circ$ , with no constraints in the  $Mult_{tot}$ . At backward angles, between  $40^\circ$  and  $60^\circ$  (see Fig.1), the spectra are enriched by a lower energy protons component, indicating moving sources which are created in the overlapping region (participant) of the nucleus-nucleus interaction and having a velocity intermediate between the projectile velocity and the target one.

In the present analysis, basically devoted to p-p correlations, we have chosen the less restrictive condition of  $Mult_{tot} > 25$  in order to take into account for a compromise between centrality selection

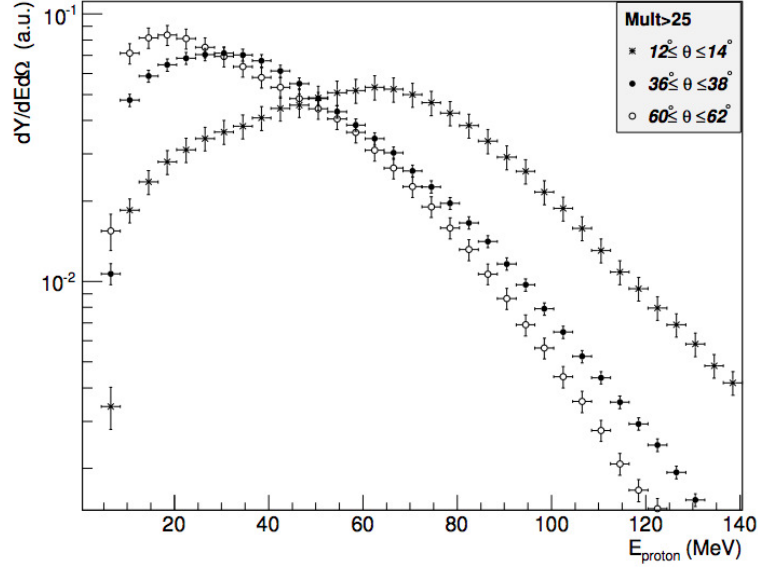


**Figure 2:** Energy spectra at three selected angular regions for  $Mult_{tot} \geq 25$  (see text for explanations) [12]

and collected statistics, useful for the data analysis. By applying this latter multiplicity condition, we can clearly see in Fig.2, that the prompt quasi-projectile component is strongly suppressed. The spectra of Fig.2 (in particular at backward angles) are interpreted as due to the presence of two possible emitting sources: a short-lived one due to a reaction stage characterized by pre-equilibrium emission, and a long-lived one (slow) due to the contribution of the late stages of the reaction (evaporations, secondary decay, etc.).

Having these selections in mind, in the following of the paper the proton-proton correlation function of the studied reaction will be discussed in some details.

### 3. Proton-proton correlation function method

In Fig.3 the proton-proton correlation function is shown (see below for the description). The experimental correlation function,  $1 + R(\mathbf{q})$ , is defined by the following equation:

$$Y_{12}(\mathbf{p}_1, \mathbf{p}_2) = C_{12} \cdot [1 + R(\mathbf{q})] \cdot Y_1(\mathbf{p}_1) \cdot Y_2(\mathbf{p}_2). \quad (3.1)$$

Where  $Y_{12}(\mathbf{p}_1, \mathbf{p}_2)$  is the yield of the two particles detected in the same event, and  $C_{12}$  is a normalization constant obtained by imposing that  $R(\mathbf{q}) \approx 0$  for very large values of the relative momentum,  $\mathbf{q}$ , of the two particles. The quantities  $Y_1(\mathbf{p}_1)$  and  $Y_2(\mathbf{p}_2)$  are the single particle yields of the two particles. Theoretically the proton-proton correlation function is evaluated by the Koonin-Pratt integral equation [9]:

$$1 + R(\mathbf{q}) = 1 + \int d\mathbf{r} S(\mathbf{r}) \cdot K(\mathbf{r}, \mathbf{q}). \quad (3.2)$$

$S(\mathbf{r})$  is the source function and it is defined as the probability to emit two protons at the relative particle-particle distance  $r$ , calculated at the time when the second proton is emitted; the function

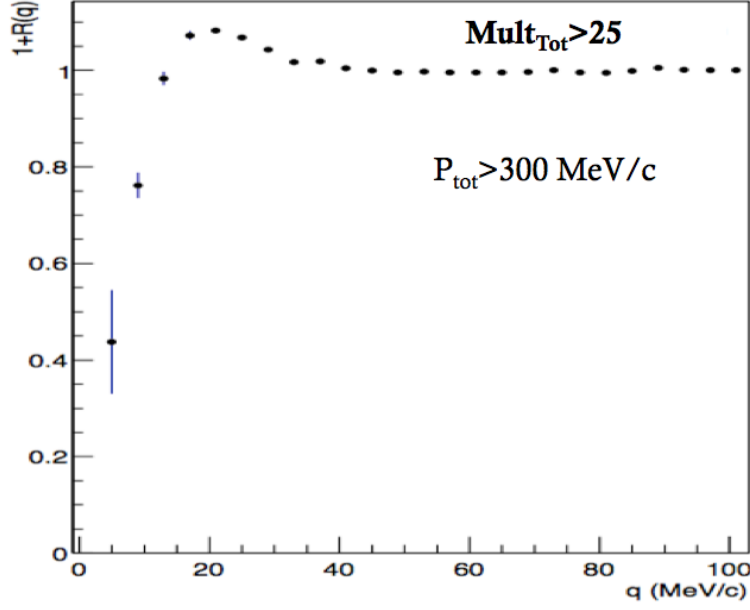


**Figure 3:** Proton-proton correlation function in Xe+Au 50 MeV/nucleon [12]

$K(\mathbf{r}, \mathbf{q})$  is the kernel of the integral equation and it contains the ingredients of the Coulomb plus Nuclear final state interactions (FSI), and quantum statistics effects (dealing with two identical fermions). As already suggested in the previous chapter, the correlation function shown on Fig.3 includes contributions of protons emitted from different stages of the collision and correspondingly to different emitting sources: a fast source, due to early dynamical emissions, and a slow, due to the evaporation of highly excited matter and to secondary decay produced by primary excited fragments.

In order to characterize the emitting source,  $S(\mathbf{r})$ , we first used a Gaussian approach, by assuming:

$$S(\mathbf{r}) \propto e^{-\frac{r^2}{2r_0^2}}. \quad (3.3)$$

To take into account the contribution of different emitting time-scales, the source function is split in two contributions schematically named "fast" and "slow", and the corresponding correlation functions calculated with Eq.(3.2) are shown in Fig.4.

The main contributions of the slow emitting source is found at low values of relative momentum ( $q < 15\text{MeV}/c$ ) where, from an experimental point of view, it is necessary to have very good resolution (essentially angular resolution) to constrain the theoretical predictions. In the experiment described in this paper, the angular resolution, about  $0.5^\circ$ , was not enough to efficiently detect pairs of protons with such a low values of the relative momentum. In order to describe the relative importance of the fast and slow components and to take into account for the difficulty in detecting pairs of protons at low values of relative momentum, a modified Gaussian source function has been used:

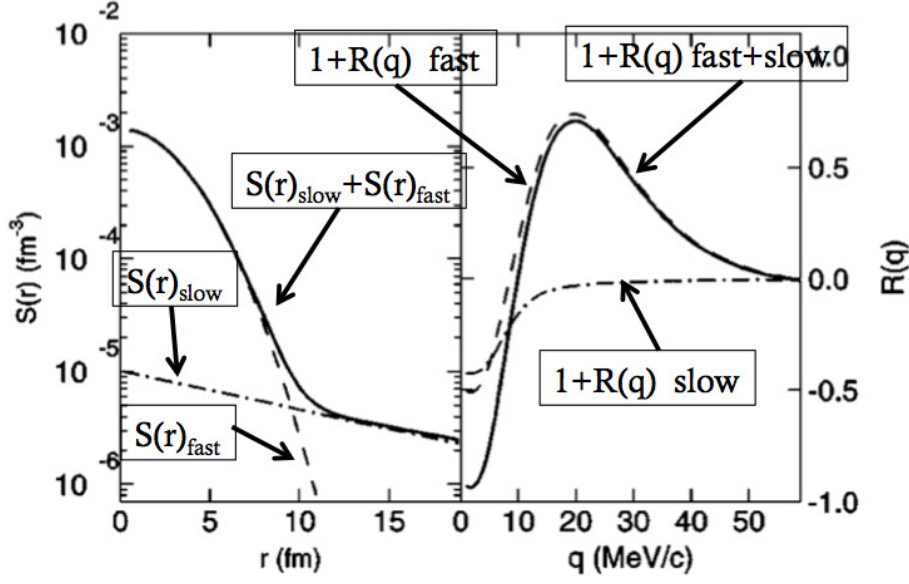


**Figure 4:** Comparison between a fast emitting source function and a slow emitting source function with their sum(left side), and their corresponding correlation functions [11] (right side)

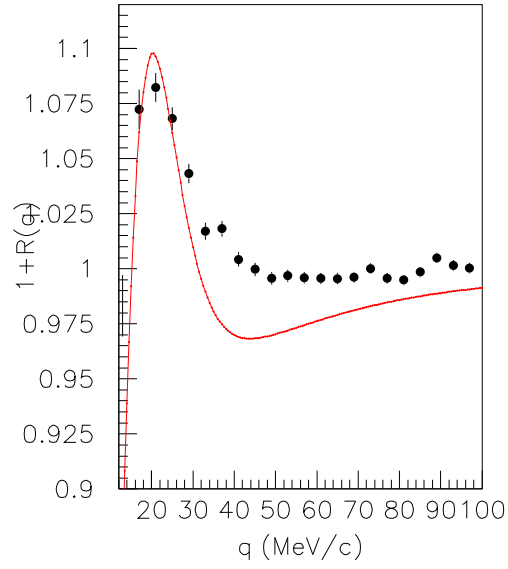
$$S(\mathbf{r}) = \frac{\lambda}{(2\pi)^{\frac{3}{2}} r_0^3} e^{-\frac{r^2}{2r_0^2}}. \quad (3.4)$$

In Eq.(3.4),  $r_0$  is the size parameter (as in Eq.(3.3)) and  $\lambda$  is the parameter describing the fraction of proton-proton pairs emitted only by the fast emitting source. In the literature the height of the correlation peak has been commonly linked to the size of the emitting source [10]. It was shown that such link is only possible if one assumes that  $\lambda = 1$ , i.e., if all proton-proton pairs were emitted by the fast emitting source [12]. We first fixed  $\lambda = 1$  and perform a best fit of the  $1+R(\mathbf{q})$  with Eq.(3.4), obtaining  $r_0 = 6.3 fm$  (see Fig.5). The quality of the fit is very poor.

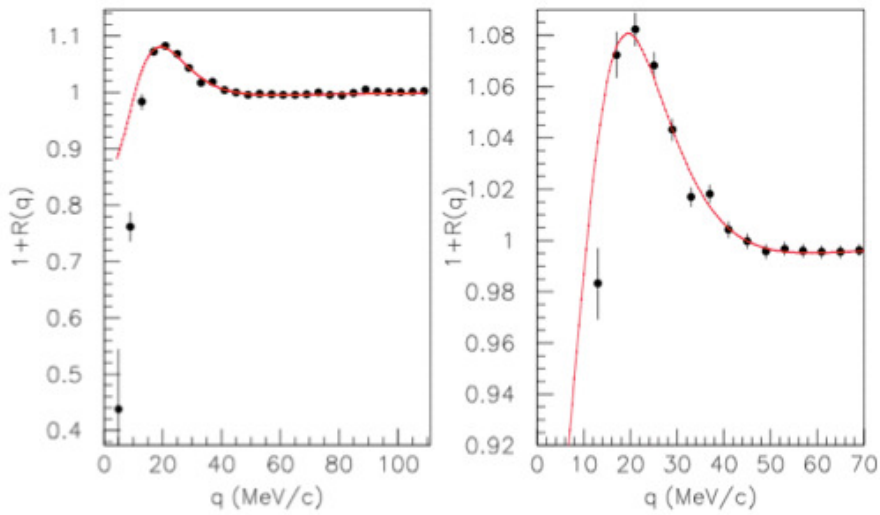
If the lambda parameter is not fixed to unity, due to overlapping sources involving with different time-scales, the peak at 20 MeV/c does not uniquely determinate the size of the source [12, 14]. For this reason, in order to extract a realistic value of the size, it is important to measure with high accuracy the overall shape of the correlation function while not fixing  $\lambda = 1$ .

Fig.6 shows a new best-fit of the data, where both  $\lambda$  and  $r_0$  are left as free parameters.

In this case a better agreement with the experimental data is clearly achieved. The  $\chi^2$  decrease from 7.45 (Fig.5) to 0.96 (Fig.6). The values of the size and of the parameter  $\lambda$  are respectively,  $r_0 = 4.1(\pm 0.4) fm$  and  $\lambda = 0.13$ . This best-fit provides a slight smaller size of the source and a strong reduction (about 15%) of the intensity of the fast component of proton-proton pairs. In order to extract physics information in a less model-dependent way, allowing for possible deviations from the commonly used gaussian profile, the analysis was pursued by applying the Imaging technique [11]. The Imaging technique consists of a numerical inversion of the Koonin-Pratt equation, Eq.(3.2). This procedure allows to extract the source function without any a priori assumptions about its shape. The result of this imaging analysis provides the profile of the source shown on the



**Figure 5:** Gaussian fits of the experimentally correlation function ( $\lambda = 1$ ) [12]



**Figure 6:** Gaussian fit of the experimentally correlation function, with  $\lambda$  parameter free, and for  $q > 20\text{MeV}/c$  [12]

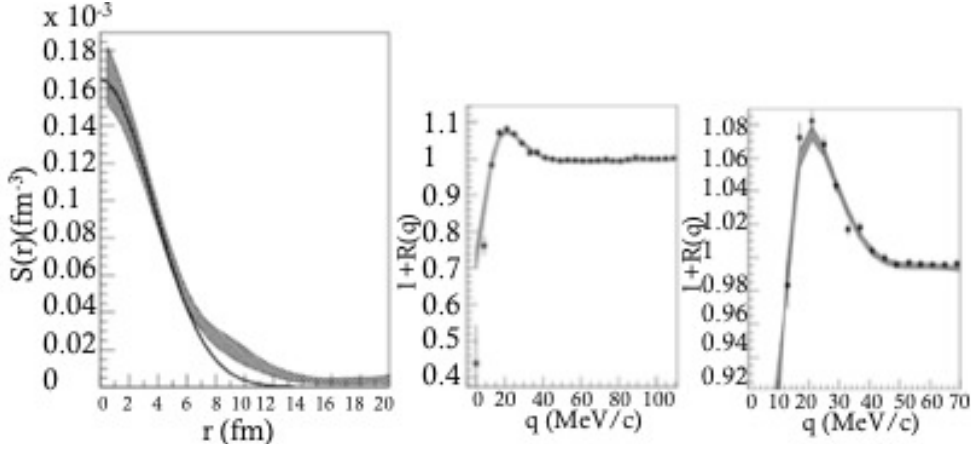


**Figure 7:** Left panel:  $S(r)$  extracting by imaging. Right panel: the corresponding correlation function describing the experimental correlation function (full dots) [12]

right size of Fig.7. The extracted profile displays a two-component behavior: a short-range portion ( $r \leq 6$ fm) which looks like a Gaussian function and long-range portion ( $r > 6$ fm) with a non-Gaussian tail which is best observed in log-scale (right panel of Fig.8) [12].

The size of the source function evaluated as the value of FWHM of the extracted profile, (Fig.7 and Fig.8), amount to  $r_{\frac{1}{2}} = 4.4(\pm 0.3)$ fm. In the Gaussian case  $r_{\frac{1}{2}} = \sqrt{2 \ln 2} r_0 = 4.8(\pm 0.4)$ . The imaging size looks like smaller than the one extracted by means of the Gaussian function assumption.

On Fig.8 we show (thin solid line) a gaussian best fit of the short range portion of  $S(\mathbf{r})$  ( $r < 6$ fm). one observes that for values of the radius  $r$  of the source profile smaller than about 6 fm the short range portions of  $S(\mathbf{r})$  shows a Gaussian profile.

Significant deviations are seen for larger values of  $r$  (long-range portion). Therefore a better fit of the data, as it is obtained by imaging, leads to a fast source profile that significantly deviates from a Gaussian shape. Its integral is given by:

$$\lambda_{fast} = 4\pi \int_0^{r_{max}} S(\mathbf{r}) r^2 dr. \quad (3.5)$$

where  $r_{max}$  is a reasonable maximum limit. For example, by choosing  $r_{max} = 2.5 r_{\frac{1}{2}}$ , we obtained  $\lambda_{fast} = 0.18$ . Even evaluating the integral up to  $r_{max} = 20$ fm or more, we obtained a values of  $\lambda$  which is of the order of 0.4 and never close to unity. This suggested also that the shape of the of energy spectra in Fig.1 revealing the presence of multiple emission mechanism and, among them, quasi-projectile evaporations [12].

A particle-particle correlation method requires the use of suitable and powerful experimental constraints in order to reduce ambiguities. In this paper we have used the total charged particle multiplicity to constraint centrality of collisions. It is desirable to use more selective observables, such as, reaction plane and transverse energy [15] that can be easily compared with theoretical simulations. This type of experiment require the use of efficient  $4\pi$  detectors [16, 17], coupled to high angular resolution devices.

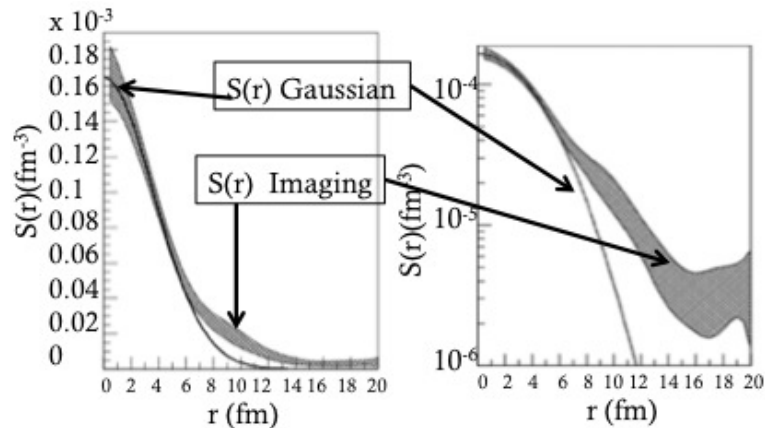


**Figure 8:** Comparison between extracted imaging source function and its Gaussian (solid line) fit within first 6 fm [12]

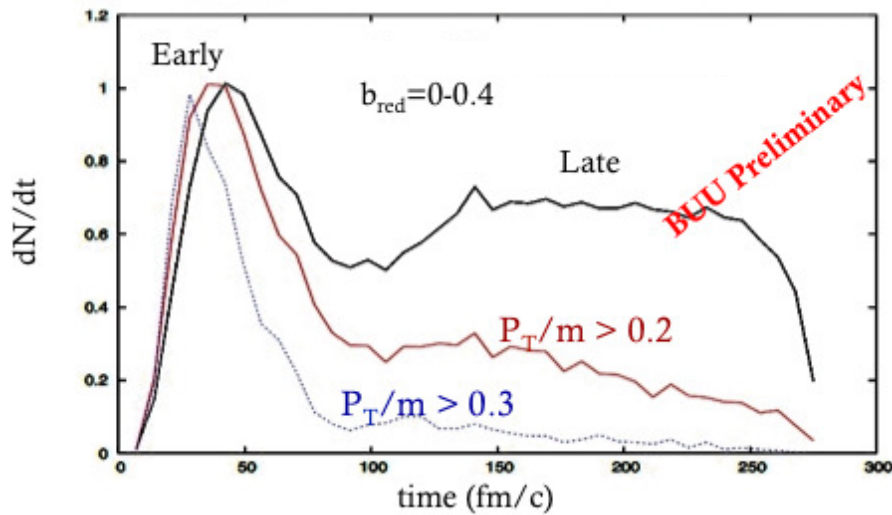


**Figure 9:** BUU simulations

We are presently using BUU model calculations to try to disentangle between protons emitted in the early stage of the reaction and the ones emitted in a later stage. In particular these simulations suggest that the transverse momentum  $P_t$  of the emitted protons can be used as an observable useful to isolate the different time scales. Fig.9 (solid black line) shows the emission rate of protons in a BUU simulation [20] of the Xe + Au at  $E/A = 50$  MeV/u and  $b_{red} < 0.4$ , as function of time. we observe two bumps corresponding to early dynamical emission (fast, at  $t$  around 50 fm/c) and to later stages (slow, at  $t > 120$  fm/c). The red solid and the blue dotted lines show the emission rate protons with high transverse momenta. This preliminary result suggest that  $P_t$  gates are dominated by protons emitted at the early stages [19, 20]. It will be interesting investigate on this aspect by studying  $P_t$  gated correlation functions [19].

## 4. Conclusions

In this paper, briefly, a particle-particle correlation analysis and its use in understanding the dynamics proton emissions in nuclear reactions is reported. It is shown that shape analysis of particle-particle correlation functions are important to disentangle among source with different time scales, ranging from dynamical and pre-equilibrium emissions to slow decay processes. A more extensive investigation of the emitting sources will require the study of correlations and imaging techniques with also including neutrons and other complex fragments. We stress the necessity to increase the resolution of particle-particle correlator arrays and integrate their use within  $4\pi$  detectors. In this perspective, we working on the construction of a new correlation array, FARCOS (Femtoscope Array for Correlations and Spectroscopy) at INFN of Catania and LNS (Laboratori Nazionali del Sud). This array is expected to extend capabilities to include also neutron detection in coincidence with CHIMERA, has allowing for the investigation of n-n and n-p correlations [18]. The similarity in the composition of FARCOS and CHIMERA stimulated the effort to extend such capabilities to both devices by adding new materials that are presently under investigations.

## References

- [1] Bao-An Li et al. Phys. Rev. C **71** 044604 (2005);
- [2] V. Baran et al. Nucl. Phys. A **730** 329 (2004);
- [3] S. Hudan et al. Phys. Rev. C **67** 064613 (2003);
- [4] T. X. Liu et al. Phys. Rev. C **69** 014603 (2004);
- [5] W. P. Tan et al. Phys. Rev. C **64** 051901 (2001);
- [6] G. Verde et al. Eur. Phys. J **A30** 81-108 (2006);
- [7] G. R. Satcheler. Introduction to Nuclear Reactions, edited by THE MACMILLAN PRESS LTD 1980, pp. 15,71 (ISBN 0-333-25907-6);
- [8] B. Davin et al. Nucl. Instr. and Meth. A **473** 302 (2001);
- [9] S.E. koonin Phys. Lett. **B 70** 43 (1977);
- [10] W. G. Gong et al. Phys. Rev. C **43** 1184 (1991);
- [11] G. Verde et al. Phys. Rev. C **65** 054609 (2002);
- [12] E. V. Pagano Tesi di Laurea Magistrale in Fisica Nucleare, A.A 2011-2012;
- [13] G. Verde et al. Phys. Rev. C **67** 034606 (2003);
- [14] E. V. Pagano in press Nuovo Cimento C- Colloquia and Communications in Physics;
- [15] R. Kotte et al. Phys. Rev. C **51** 2686 (1995);
- [16] A. Pagano et al. Nuc. Phys. A **734** 504 (2004);
- [17] J. Pouthas et al. Nucl. Instr. and Meth. A **357** 418 (1995);
- [18] R. Ghetti et al. Phys. Rev Lett. **87** 2710 (2001);
- [19] T. Minniti PhD Thesis, A.A 2012-2013;
- [20] B. Barker NSCL PhD Thesis, 2013;